

## DOMAIN STRUCTURES OF EPITAXIAL SrRuO<sub>3</sub> THIN FILMS

J. C. JIANG \*, X. PAN \* and C. L. CHEN \*\*

\*Department of Materials Science and Engineering, The University of Michigan, Ann Arbor, MI 48109

\*\*Texas Center for Superconductivity and Department of Physics, University of Houston, Houston, TX 77204

### ABSTRACT

The structural characteristics of SrRuO<sub>3</sub> thin films deposited on a (001) SrTiO<sub>3</sub> substrate by pulsed laser were studied by transmission electron microscopy (TEM) and high-resolution TEM. TEM studies of cross-sectional specimens revealed the epitaxial growth of the films with the SrRuO<sub>3</sub>-(110) plane parallel to the SrTiO<sub>3</sub>-(001) plane. Two types of 90° rotational domain structures were observed in both cross-sectional and plan-viewing specimens. The in-plane orientations of these domains with respect to the substrate are either of SrRuO<sub>3</sub>-[ $\bar{1}$ 10] // SrTiO<sub>3</sub>-[100] and SrRuO<sub>3</sub>-[001] // SrTiO<sub>3</sub>-[010], or of SrRuO<sub>3</sub>-[1 $\bar{1}$ 0] // SrTiO<sub>3</sub>-[010] and SrRuO<sub>3</sub>-[001] // SrTiO<sub>3</sub>-[100].

### INTRODUCTION

Epitaxial thin films of SrRuO<sub>3</sub> have been found useful for making devices such as electrodes and junctions in microelectronic devices due to the high resistance to chemical corrosion and outstanding thermal conductivity and stability. Recently, crystalline thin films of high quality were reported to be successfully grown on different substrate materials by different methods in different groups, such as on SrTiO<sub>3</sub> (100) and LaAlO<sub>3</sub> (100) by 90° off-axis sputtering technique [1], on LaAlO<sub>3</sub> (100) [2] and on SrTiO<sub>3</sub> (001) [3-5] by pulsed laser ablation. Single domain and multi-domain structures were reported to be present in thin films grown on different misoriented (001) SrTiO<sub>3</sub> substrates [6]. However, to our knowledge, detailed studies on the structural characteristics of these films have not yet been reported. Since surface morphology, microstructure, interfaces and defects in thin films affect the properties of devices, it is important to examine the quality of the films and to characterize their microstructures. In the present work, we report a TEM study of the SrRuO<sub>3</sub> films prepared by pulsed laser ablation method.

SrRuO<sub>3</sub> belongs to ternary ruthenium oxide system that includes compounds like CaRuO<sub>3</sub>, BaRuO<sub>3</sub> and Sr<sub>2</sub>RuO<sub>4</sub> [7,8]. It is a distorted, pseudo-cubic perovskite structure [8] and was reported to be an orthorhombic phase of GdFeO<sub>3</sub> type [9]. The space group was determined to be Pbnm (No. 62) and lattice parameters  $a=5.5670$  Å,  $b=5.5304$  Å and  $c=7.8446$  [10]. It is paramagnetic and metallic conductive at room temperature [11] and ferromagnetic below ~160K [7].

### EXPERIMENTAL

SrRuO<sub>3</sub> thin films were deposited on (001)-SrTiO<sub>3</sub> by means of pulsed laser ablation. Details on the deposition process were described in the literature [3]. Cross-section slices were obtained by cutting SrRuO<sub>3</sub>/SrTiO<sub>3</sub> along the [100] or [010] directions of SrTiO<sub>3</sub>, and then were glued face to face by joining SrRuO<sub>3</sub> film surfaces. Specimens for both cross-section and plan-view TEM studies were prepared by mechanical grinding, polishing and dimpling followed by Ar-ion milling using a Gatan Precision Ion Polishing System (PIPS™, Model 691, Pleasanton, CA) at 5 kV at an angle of 6°. Electron diffraction patterns and dark field images were taken in a Philips EM420 electron microscope operated at 100 kV. High-resolution transmission electron microscopy (HRTEM) studies were conducted with a JEOL 4000EX microscope, operated at 400 kV, which provides a point resolution of ~0.17 nm.

## RESULTS AND DISCUSSION

Figure 1(a) is a dark-field image of a cross-sectional sample, formed by using a reflection of the SrRuO<sub>3</sub> film, showing the morphology of a SrRuO<sub>3</sub> film on SrTiO<sub>3</sub>. The film has a flat surface and sharp interface and maintains a uniform thickness of 150 nm over the entire specimen. The surface roughness is approximately a few nanometers in height. HRTEM studies of cross-sectional specimens showed that the interface between the film and the substrate has good lattice matching. An example of the interfacial structure is shown in Fig. 1(b). Note that the upper and lower parts of the SrRuO<sub>3</sub> film in Fig. 1(a) show different contrasts. Figure 1(c) and 1(d) are the selected-area electron diffraction (SAED) patterns taken from the lower (bright) and the upper (dark) regions of the SrRuO<sub>3</sub> film in Fig. 1(a), respectively, for which the electron beam direction is nearly parallel to the [100] axis of the SrTiO<sub>3</sub> substrate. Figure 1(c) is identified to be the [110] electron diffraction pattern of the SrRuO<sub>3</sub> structure, in which the  $[1\bar{1}0]$  direction is parallel to the normal of the as-grown film surface, i.e. the growth direction, while the [001] direction is located

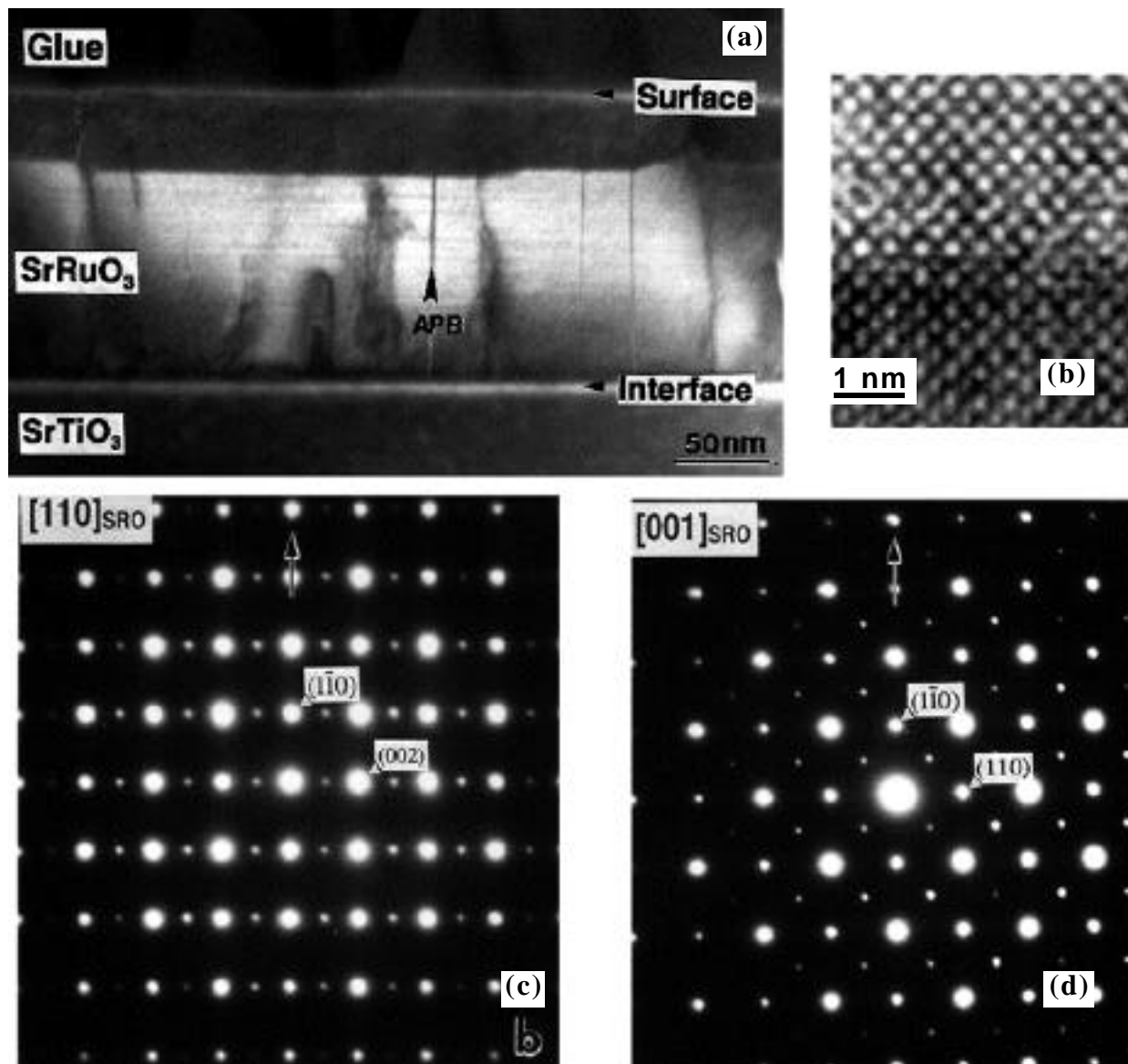


Figure 1 (a), Dark-field image using the  $(1\bar{1}1)$  reflection of SrRuO<sub>3</sub> showing two-type domain structures (white and black). Dark straight lines (marked by an arrow) within the white regions are antiphase boundaries (APBs). (b) and (c) SAED patterns from the white and black regions showing the [110] and [001] zone of SrRuO<sub>3</sub>, respectively.

in the film plane. Figure 1(d) is the [001] electron diffraction pattern of the  $\text{SrRuO}_3$  structure, which again shows that the growth direction of the film is along the [110] direction instead of the [001] direction proposed previously [3]. This conclusion was further confirmed by studying the electron diffraction patterns when tilting the TEM specimen. By tilting the specimen around the growth direction from the [110] zone SAED (figure 1(c)) through  $90^\circ$ , the [001] zone electron diffraction pattern, as shown in figure 1(d) will be obtained, and vice versa.

From electron diffraction patterns of the  $\text{SrRuO}_3$  films shown above it also can be concluded that the  $\text{SrRuO}_3$  thin film consists of domains with two different orientations (Fig. 1(c) and 1(d)) with respect to the substrate. The two domain structures can be clearly revealed and distinguished using dark-field imaging. In fact, the image in Fig. 1(a) was obtained by using the  $(1\bar{1}1)$  reflection in Fig. 1(c). Therefore, the upper part of the film in Fig. 1(a) appears dark, while the lower part appears bright. According to the electron diffraction patterns in Fig. 1(c) and 1(d), the two types of domains are rotated with respect to each other by  $90^\circ$  around the [110] growth direction.

The  $90^\circ$  rotation domain structures in  $\text{SrRuO}_3$  films were also observed in the plan-view images. Figure 2(a) shows a SAED pattern taken from a plan-view specimen of the same film as

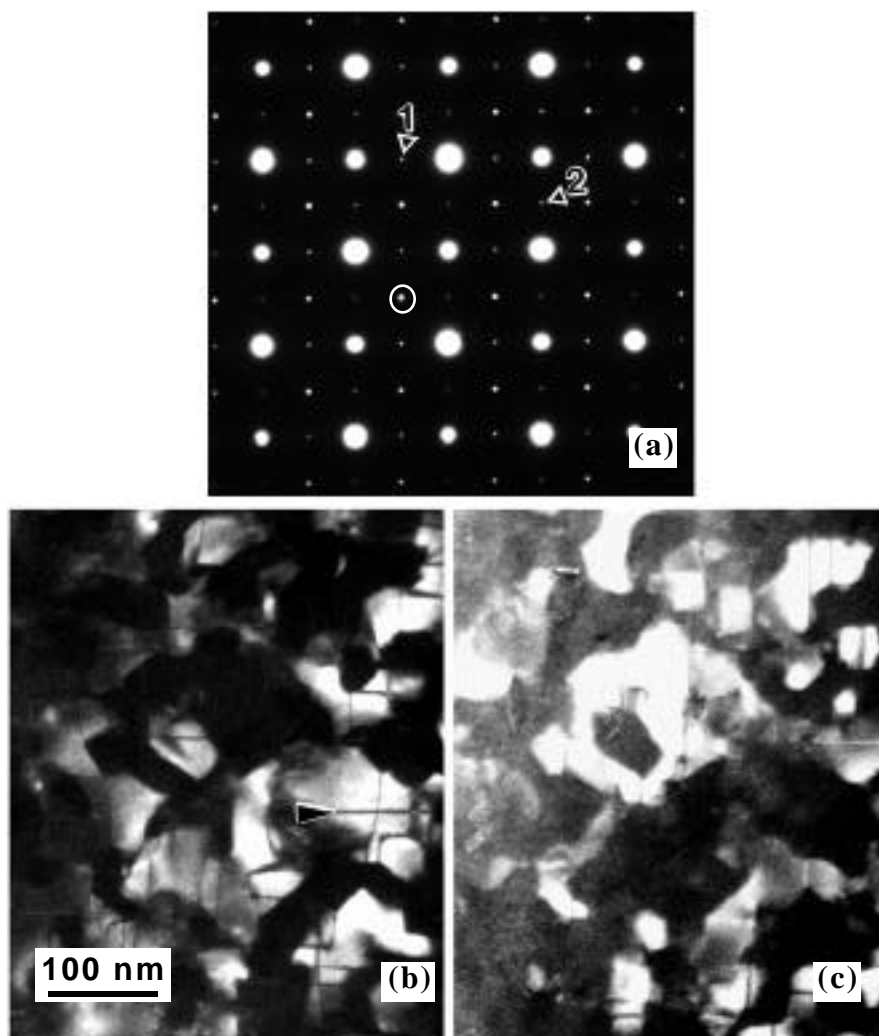


Figure 2 (a), A SAED pattern taken from a plan-viewing specimen showing a superposition of two  $90^\circ$  rotational [110] zone SAED patterns. (b) and (c) are dark-field images obtained by using the weak reflections “1” and “2” in (a), respectively. Fine dark straight lines (marked by arrows) in (b) and (c) are APBs.

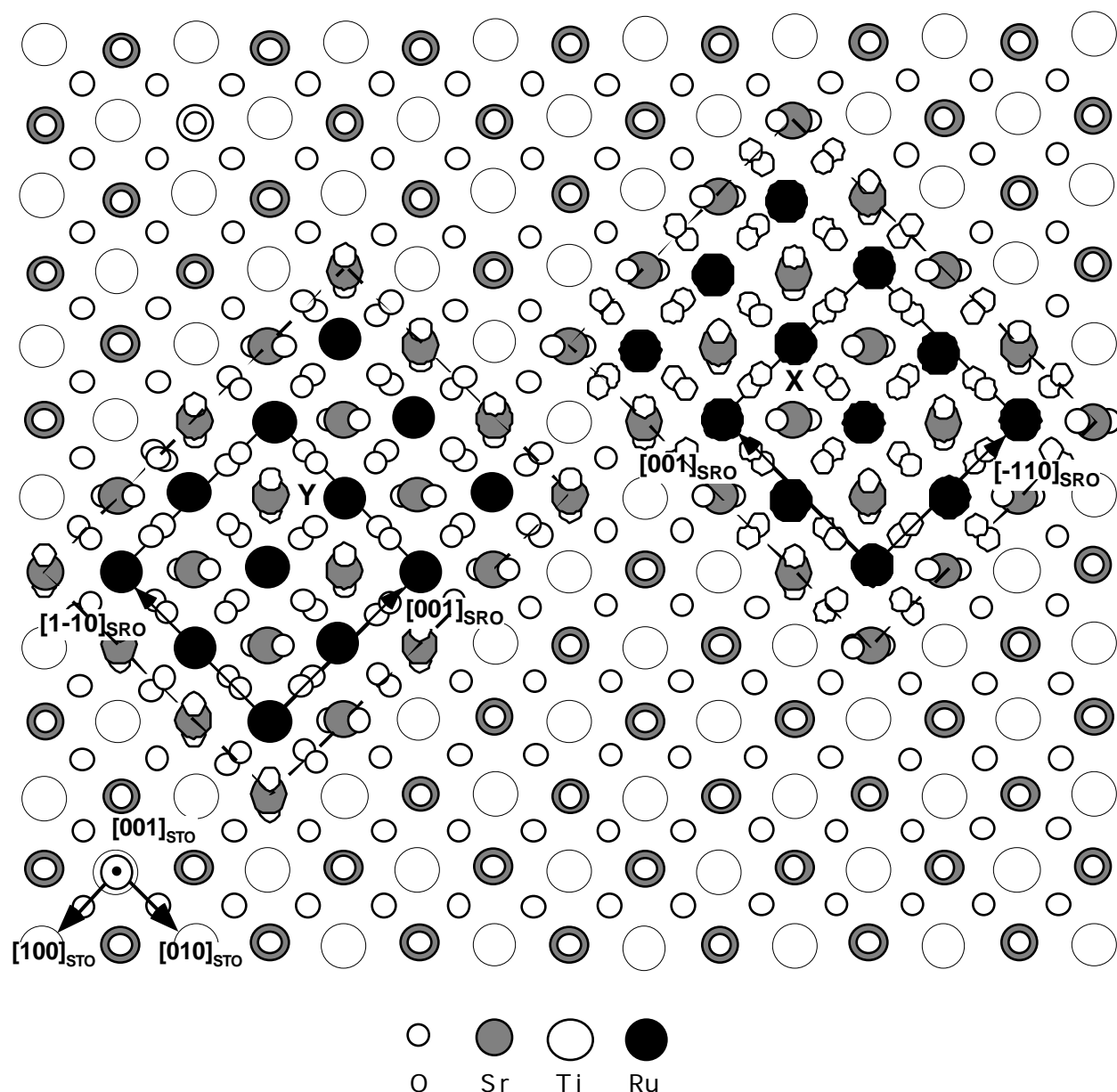


Figure 3. Schematic diagram showing the 90° rotation of the two type domains (X and Y) and their in-plane orientation relationship with respect to the substrate SrTiO<sub>3</sub>. In region X: SrRuO<sub>3</sub>  $[\bar{1}10] \parallel \text{SrTiO}_3 [100]$  and SrRuO<sub>3</sub>  $[001] \parallel \text{SrTiO}_3 [010]$ , In region Y, SrRuO<sub>3</sub>  $[1\bar{1}0] \parallel \text{SrTiO}_3 [010]$  and SrRuO<sub>3</sub>  $[001] \parallel \text{SrTiO}_3 [100]$ .

for the cross-sectional TEM studies in Fig. 1. It shows different features from the  $[001]$  electron diffraction pattern (compare with the image in Fig. 1(d)). This diffraction pattern is a superposition of two  $[110]$  diffraction patterns that are rotated around the zone axis with respect to each other by 90°. Reflections such as the one circled in Fig. 2(a), which are located in the center of the square formed by four strong reflections, result from double diffraction from the two types of 90° rotation domains. The domains with different orientations can be clearly distinguished by dark-field imaging. Fig. 2(b) and 2(c) are the dark-field images, obtained by using the weak reflections “1” and “2” in Fig. 2(a), respectively, which belong to two different  $[110]$  zone electron diffraction patterns. The dark and bright regions in the images represent two different domains. The contrasts in these two images are reversed, which indicate that the SrRuO<sub>3</sub> thin film consists of only these two 90° rotation domains. In addition, fine dark straight lines (marked by arrows in Fig. 2(b) and 2(c)) within each domain are APBs, similar to those shown in Fig. 1(a).

The orientation relationship between the two type domains (X and Y) and their in-plane orientation relationship with respect to the substrate SrTiO<sub>3</sub> can be summarized in figure 3.

SrRuO<sub>3</sub> films growing in the [110] direction deviates from the accepted models. However, by considering the possible interfacial structural model of SrRuO<sub>3</sub>/SrTiO<sub>3</sub>, we find that this is reasonable. Assume that the SrRuO<sub>3</sub> films grow with its *c*-axis normal to the SrTiO<sub>3</sub> (001) surface. Then the in-plane orientation relationship is: SrRuO<sub>3</sub> [100] // SrTiO<sub>3</sub> [110] and SrRuO<sub>3</sub> [010] // SrTiO<sub>3</sub> [1  $\bar{1}$  0]. The lattice mismatches along the SrRuO<sub>3</sub> [100] and [010] directions are equal to 0.14% and 0.81%, respectively, as calculated using the formula given in the literature [3]. Similarly, if the SrRuO<sub>3</sub> film grows with its [110] axis normal to the SrTiO<sub>3</sub> (001) surface, then the in-plane orientation relationship is: SrRuO<sub>3</sub> [ $\bar{1}$  10] // SrTiO<sub>3</sub> [100] and SrRuO<sub>3</sub> [001] // SrTiO<sub>3</sub> [010]. The lattice mismatches along the SrRuO<sub>3</sub> [ $\bar{1}$  10] and [001] directions are equal to 0.44% and 0.47%, respectively. By comparing these two possible models, we find that the strain field from the lattice mismatch is more isotropic for the latter case than for the former case. Therefore, it is likely that the growth of SrRuO<sub>3</sub> films along the [110] axis is more favorable.

The mechanism for the formation of such domain structures is not yet clear. There are some results reported in the literature [6] that the misorientation of the substrate is responsible for the formation of the single crystalline thin films. It can be predicted that surface properties, such as orientation of the substrate, roughness, steps, kinks and even surface reconstruction may play an important role in the growth of single crystal films. Detailed studies of SrRuO<sub>3</sub> thin films grown on SrTiO<sub>3</sub> substrates with different degrees of misorientations from the (001) planes are in progress.

## CONCLUSIONS

In summary, thin films of SrRuO<sub>3</sub> produced by pulsed laser deposition were proved to be epitaxially grown on (001) SrTiO<sub>3</sub> along the [110] directions, with rather good lattice-matching to the substrate. Two types of 90° rotational domain structures in the film were observed. Each type of domain has an in-plane orientation relationship with respect to the substrate of either SrRuO<sub>3</sub> [ $\bar{1}$  10] // SrTiO<sub>3</sub> [100] and SrRuO<sub>3</sub>[001] // SrTiO<sub>3</sub>[010], or SrRuO<sub>3</sub>[1  $\bar{1}$  0] // SrTiO<sub>3</sub>[010] and SrRuO<sub>3</sub>[001] // SrTiO<sub>3</sub>[100].

## ACKNOWLEDGMENTS

The authors wish to thank Mr. Eric Wang (Materials Science & Engineering, University of Michigan) for his assistance during specimen preparation. This work was supported by the college of Engineering, the University of Michigan.

## REFERENCES

1. C. B. Eom, R. J. Cava, R. M. Fleming, J. M. Philips, R. B. van Dover, J. H. Marshall, J. W. P. Hsu, J. J. Krajewski and W. F. Peck, Jr., *Science* **258**, 1768 (1992).
2. X. D. Wu, S. R. Foltyn, R. C. Due and R. E. Muenchausen, *Appl. Phys. Lett.* **62**, 2434 (1993).
3. C. L. Chen, Y. Cao, Z. J. Huang, Q. D. Jiang, Z. H. Zhang, Y. Y. Sun, W. N. Kang, L. M. Dezaneti, W. K. Chu and C. W. Chu, *Appl. Phys. Lett.* **71**, 1047 (1997).
4. J-P. Maria, S. Trolier-Mckinstry, D. G. Schlom, (Mat. Res. Soc. Proc. 474, Pittsburgh, PA, 1997), p. 217-222.
5. A. F. Marshall, L. Klein, C. H. Ahn, S. Dodge, J. Reiner, L. Antognazza, L. Mieville, A. Kapitulnik, T. H. Geballe, and M.R. Beasley, (Mat. Res. Soc. Proc. 474, Pittsburgh, PA, 1997), p. 223-228.
6. Q. Gan, R. A. Rao and C. B. Eom, *Appl. Phys. Lett.* **70**, 1962 (1997).
7. A. Callaghan, C. W. Moeller and R. Ward, *Inorg. Chem.* **5**, 1572 (1966).
8. J. Randall and R. Ward, *J. Am. Chem. Soc.* **81**, 2629 (1959).

9. S. Geller, *J. Chem. Phys.* **24**, 1236 (1956).
10. C. W. Jones, P. D. Battle, P. Lightfoot and W. T. A. Harrison, *Acta Cryst.* **C45**, 365 (1989).
11. R. J. Bouchard and J. L. Gillson, *Mater. Res. Bull.* **7**, 873 (1972).